

Evidence for a depinning transition in the vortex quasilattice of $\text{Bi}_2\text{Sr}_2\text{CaCu}_2\text{O}_{8+\delta}$

C. D. Dewhurst and R. A. Doyle

Interdisciplinary Research Centre in Superconductivity, University of Cambridge, Cambridge CB3 0HE, United Kingdom

(Received 7 May 1997)

Magnetization measurements have been performed on several crystals of $\text{Bi}_2\text{Sr}_2\text{CaCu}_2\text{O}_{8+\delta}$ as a function of both temperature and magnetic field. A pinning crossover for vortices is identified at fields above the arrowhead second peak transition but below the irreversibility line in agreement with recent Hall-array measurements. In addition, a small but clear feature is apparent in the derivative of the magnetic moment as a function of temperature at fields below that of the arrowhead at an almost field-independent temperature of about 32 K. These features define a pinning-related transition that crosses continuously from the disordered into the ordered vortex solid phase. [S0163-1829(97)02641-6]

$\text{Bi}_2\text{Sr}_2\text{CaCu}_2\text{O}_{8+\delta}$ (BSCCO) is a model system for the study of the generic vortex behavior in anisotropic high-temperature superconductor (HTS) materials.¹ The large anisotropy, unusual parameter values, and strong thermal activation effects conspire to make bulk pinning very weak over a wide range of reduced temperature.² At the same time, pronounced surface^{3,4} and geometrical effects⁴⁻⁶ result in hysteresis in the magnetic moment, in addition to that from bulk pinning, and obscure or complicate clear identification of the various transitions or crossovers in the H - T phase diagram. Thus, the complete magnetic phase diagram for BSCCO remains a subject of ongoing interest. Small angle neutron scattering (SANS) and Bitter decoration measurements⁷⁻⁹ show the existence of a well-formed three-dimensional (3D) quasilattice or Bragg glass¹⁰ at low fields and temperatures in BSCCO. At high temperatures, where pinning is negligible, the vortex lattice simultaneously melts and decouples.¹¹⁻¹³ At intermediate temperatures bulk pinning becomes significant and the effects of surface barriers also become pronounced.⁴ The effect of disorder on the phase transitions and phase diagram has recently received considerable attention^{10,13,14} although the relationship between the phase transitions, irreversibility line, and the depinning line for vortices is not yet absolutely established. Zeldov *et al.*⁴ have used local Hall probe measurements to determine the onset, with increasing field, of a critical state at the temperatures where the second peak in the magnetic moment, or 'arrowhead' feature, is observed. They find a 'depinning transition' which has a weak temperature dependence and lies below the irreversibility line which is determined at these temperatures by the surface barrier.⁴ This depinning transition was observed at fields above the arrowhead only (50 mT) and indicates the temperature where the disordered 2D vortex solid or glass becomes unpinning. It is known that the vortex lattice or solid is unpinning at high temperatures,⁶ but strongly pinned below about 20 K. However, there have been no clear attempts so far to elucidate the depinning line for the vortex lattice which these two results suggest should exist. In this paper we present evidence for this depinning transition or crossover.

Samples of $\text{Bi}_2\text{Sr}_2\text{CaCu}_2\text{O}_{8+\delta}$ were obtained from two different sources.^{15,16} The as-produced mosaics were repeatedly cleaved until single, optically smooth crystals were ob-

tained with dimensions 0.5 mm^2 in the ab plane and thickness of between 10 and $20 \mu\text{m}$. Magnetic moment measurements were made as a function of temperature (m - T) or applied field (m - H) with $B\parallel c$ using a vibrating sample magnetometer. The m - T curves were measured in applied dc fields of between 1.5 mT and 5 T after either cooling to 5 K in zero applied field, applying the field, and measuring the moment during warming (FW) to 125 K, or field cooling (FC) to 5 K during measurement. Several crystals from each source were measured and the results confirmed to be general. In what follows we present results for one crystal from each source, hereafter referred to as W1 (Ref. 15) and K1 (Ref. 16). The T_c of the crystals as measured from the sharp onset of a diamagnetic signal in 0.5 mT were very close and $T_c \approx 89 \text{ K}$.

Figure 1 shows representative m - H and m - T data for crystal W1. Figure 1(a) shows the m - H curve measured at a temperature of 30 K. At this temperature, which is above the temperature interval where the arrowhead feature is observed for this crystal (22–28 K),¹⁷ the magnetic moment exhibits weak, asymmetric hysteresis becoming fully reversible above a criterion determined irreversibility field, $H_{ir} \approx 550 \text{ mT}$. The asymmetry in the m - H behavior shows that surface or geometrical barrier effects are significant since pinning always produces symmetric hysteresis. However, the remanent moment, m_{rm} , determined from the zero field intercept of the decreasing field cycle, is also marked in Fig. 1(a). This suggests that pinning effects are finite at low fields and allows the magnitude of these effects to be estimated.

Figure 1(b) shows representative m - T data for the same crystal. Both FW and FC curves at a fixed applied field of 50 mT are shown. FW and FC conditions generate different field profiles in the sample when pinning effects are significant and are often used to identify the irreversibility temperature, T_{ir} , at constant field. In the presence of bulk pinning the measured FC magnetization curve is determined by the competition between Meissner expulsion and pinning effects which prevent complete flux exclusion.^{18,19} FW measurements, on the other hand, probe the penetration of vortices, both due to increasing thermal activation and temperature dependence of the superconducting parameters as the tem-

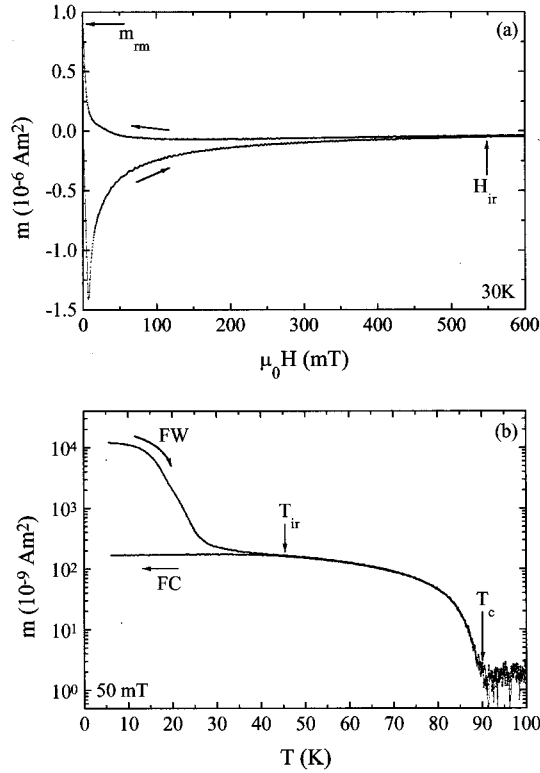


FIG. 1. Magnetic moment of crystal W1 measured as a function of (a) field at 30 K and (b) temperature at 50 mT. The irreversibility field, $H_{ir}(T)$, and temperature, $T_{ir}(H)$, are marked accordingly.

perature is raised.¹⁹ We emphasize that the regime in which most of our conclusions are drawn is at reduced temperatures where the temperature dependence of the superconducting parameters is not a significant effect.

To elucidate subtle changes in the magnetic moment with temperature we evaluate the logarithmic derivative, $S_T = d \ln(m)/dT = 1/m \, dm/dT$, of the data. Figures 2(a) and 2(b) present FW data at fields of 40 and 200 mT, respectively. These fields are larger than that at which the arrowhead feature is observed for this crystal (30 mT).¹⁷ It is clear from this figure that the derivative of the magnetic moment depends strongly on temperature at these fields and exhibits two minima indicating points of maximum slope in the $\ln(m)$ - T curve. The locus of the lower temperature minimum in S_T is associated with the temperature at which the penetrating critical state reaches the sample center.¹⁹ The higher-temperature minimum in S_T is associated with a decrease in the nonequilibrium magnetic moment as the effects of pinning are reduced due to thermal activation. The temperature at which this second minimum in S_T is observed is still considerably lower than the barrier-determined irreversibility temperature, T_{ir} , at these fields. This suggests that depinning of vortices begins at a temperature considerably lower than the irreversibility temperature, in agreement with the results of local Hall probe measurements.⁴ We therefore identify the extrapolated higher temperature end point of this “depinning peak,” T_{d1} , with a depinning temperature for the disordered vortex solid. Comparison of Figs. 2(a) and 2(b) shows that the depinning and irreversibility temperatures, T_{d1} and T_{ir} , become closer as the applied field is increased. This can be understood by the increasing role of bulk pinning relative to

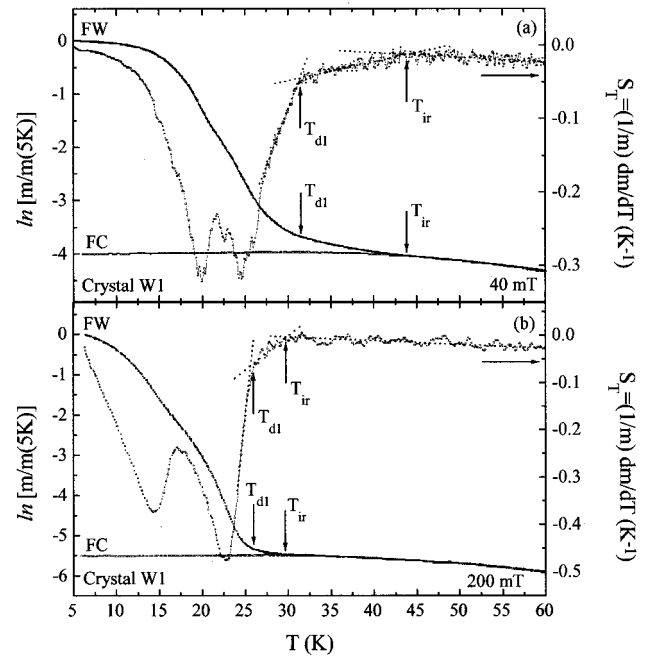


FIG. 2. Variation of the FW magnetic moment and derivative of $\ln(m)$ for crystal W1 at (a) 40 and (b) 200 mT. A depinning temperature, T_{d1} , separate from T_{ir} , is determined from the high-temperature endpoint of the “depinning” peak in S_T as marked in the figure.

surface and geometrical barrier effects as T_{d1} and T_{ir} move to lower temperatures with increasing field. $T_{d1}(H)$ and $T_{ir}(H)$ are plotted on the H - T phase diagram presented in Fig. 4(b) and are discussed further below.

Next we discuss the low field behavior below the arrowhead. The FW m - T data at an applied field of 10 mT for crystals W1 and K1 is presented in Fig. 3. The logarithmic derivative of the m - T data, S_T , exhibits a single pronounced minimum which develops with increasing field into the lower temperature minimum observed at higher fields (Fig. 2). In contrast to the high field behavior presented in Fig. 2, however, S_T does not exhibit a second “depinning” peak. Rather, a different feature is apparent in the data at a temperature $T_{d2} \approx 32$ K for both crystals. The sharp change in S_T at T_{d2} reflects a sharp change in gradient of the $\ln(m)$ - T curve. We suggest that this point marks a crossover from pinning to a surface or geometrical barrier controlled behavior.⁴⁻⁶ This is supported by the exponential variation of the low field FW magnetic moment above T_{d2} which is consistent with that expected for thermal activation of vortices over a surface barrier^{20,21} and yields comparable exponents with Ref. 4. The penetration of vortices through the surface barrier is expected to be influenced strongly by the order and dimensionality of the vortex solid phase into which they penetrate.²² In the 3D regime, penetrating vortices create surface interstitial defects in the vortex lattice which must adjust to restore equilibrium.²² Pinning of the 3D vortex lattice, however, is expected to retard this adjustment, thereby increasing the effective barrier to vortex penetration.²² This results the “softening” of the temperature dependence of the magnetic moment at temperatures just below T_{d2} and ex-

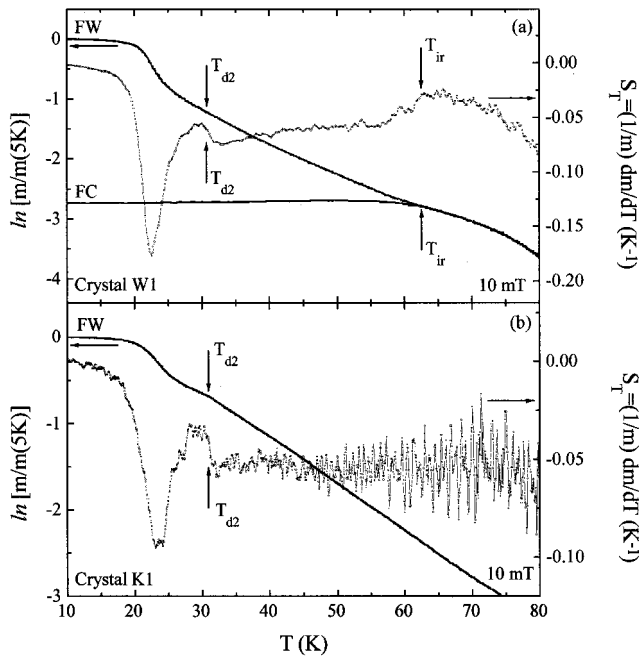


FIG. 3. Variation of the FW magnetic moment and derivative of $\ln(m)$ at 10 mT for crystals (a) W1 and (b) K1. A sharp change in gradient of the $\ln(m)$ - T curves is evident at a temperature $T_{d2} \approx 32$ K.

plains the different forms of the depinning features in the two regimes.

Further evidence for a change in the low field vortex behavior at T_{d2} is found from the remanent moment.^{17,23} The average internal magnetic field, B_{rem} , is determined from m_{rm} and the crystal dimensions and is shown as a function of temperature in Fig. 4(a). The temperature dependence of B_{rem} is rather similar to the low field m - T data measured directly (Fig. 3). In particular, the data show a similar sharp feature at $T_{d2} \approx 30$ K. The internal field at which this anomalous feature is observed is considerably smaller than the arrowhead field for this crystal (30 mT), confirming that the observed feature at T_{d2} is associated with the behavior of the low field vortex lattice phase.⁷⁻⁹ It is important to note that the low field m - T behavior in Fig. 2 and the remanent moment reflect two different processes; the former is determined by the entry of flux into the sample whilst the latter is determined by flux exit. This implies that the change in vortex behavior at T_{d2} represents a crossover which is insensitive to the direction of flux motion, i.e., due to bulk pinning rather than surface or geometrical barriers. Nideröst *et al.*²³ have measured the relaxation of the remanent moment with time over a wide temperature range and find that m_{rm} exhibits a similar change in behavior at ≈ 30 K.

The loci of the characteristic temperatures, T_{d1} and T_{d2} , identified from Figs. 1–3 are presented in Fig. 4(b). The line denoted B_{ir} marks the irreversibility line determined from the disappearance of hysteresis in both the m - H (Ref. 17) and m - T behaviors. The line denoted B_m marks the melting line determined by Zeldov *et al.*²⁴ It forms an almost continuous low field boundary with the arrowhead feature, B_{ah} , at lower temperatures showing that our crystals have similar anisotropy to that in Ref. 24. The high field depinning locus, T_{d1} , (solid circles) determined here by *global* magnetization is

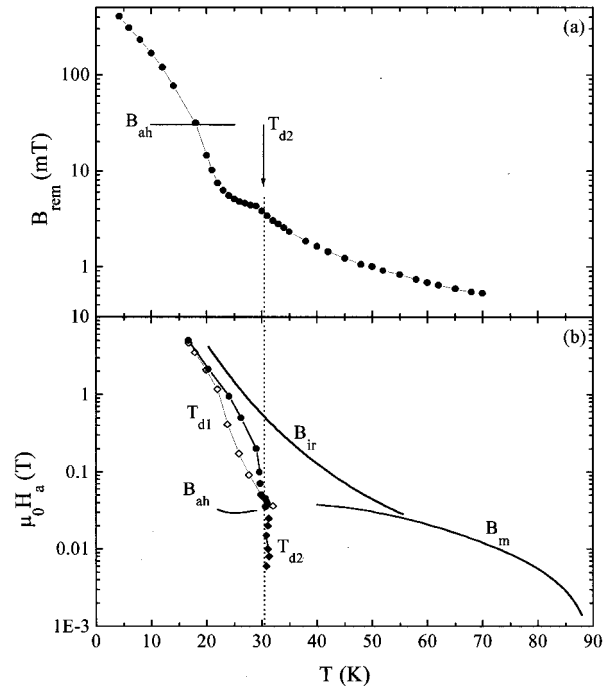


FIG. 4. (a) Average internal remanent field, B_{rem} , vs temperature. (b) Magnetic phase diagram for $\text{Bi}_2\text{Sr}_2\text{CaCu}_2\text{O}_{8+\delta}$. The boundaries T_{d1} [solid circles, this work, open diamonds, Zeldov *et al.* (Ref. 4)] and T_{d2} (solid diamonds) represent depinning boundaries of the 2D disordered vortex solid phase at high fields and 3D vortex lattice phase at low fields, respectively. B_{ir} is the irreversibility line determined where hysteresis in the m - T and m - H magnetic moment disappears. B_{ah} indicates the position of the arrowhead or second peak in the m - H behavior (Ref. 17). B_m is the melting line as determined by Zeldov *et al.* (Ref. 24).

compared with that determined by Zeldov *et al.*⁴ by local Hall probe techniques (open diamonds). They show good agreement considering small differences in intrinsic disorder in the crystals which might reasonably be expected. The locus of T_{d2} merges smoothly with the high field boundary T_{d1} . This suggests that the two boundaries represent a single continuous pinning crossover for both the low field 3D vortex lattice phase and the disordered 2D phase above it.

It is interesting to note that the depinning boundary crosses the melting and decoupling line close to where Majer *et al.*² suggest that a thermodynamic multicritical point exists. This is consistent with the suggestion that the arrowhead is a disorder driven transition.²⁵ However, it makes it less likely that the near vertical “glass transition” rising out of the critical point is a true thermodynamic transition.

The existence of a depinning boundary at a temperature well below the melting line is consistent with the conclusions that the hysteresis in the magnetic moment and critical current density above the depinning temperature is almost entirely due to surface or geometrical barriers.^{2-4,6} Our observations are not necessarily inconsistent with those of Zeldov *et al.*⁴ and Majer *et al.*⁶ who observe domelike field profiles due to the geometrical barrier in the same temperature regime at fields below where the arrowhead is observed. This only shows that bulk pinning below the arrowhead is weak and susceptible to flux creep, but cannot preclude finite pinning effects.

Finally, it is rather interesting that the proposed depinning boundary at low fields occurs in a small temperature window (≈ 1 K). The existence of a quasilattice in the temperature and field regime below the arrowhead and melting line in BSCCO (Refs. 7–9) implies that vortex-vortex interactions, rather than pinning, dominate the behavior in this regime. Thus, when pinning becomes inactive, large parts of the lattice are able to rearrange simultaneously, thereby explaining the sharp feature.

In conclusion, the temperature dependence of the FW, FC, and remanent magnetic moment has been investigated as a function of applied magnetic field. The behavior exhibits significant differences for applied fields above and below the arrowhead and/or melting field. Above this field, the logarithmic derivative of the magnetic moment exhibits a broad peak at intermediate temperatures suggesting gradual thermal de-pinning of vortices as the temperature is raised. The high temperature end-point of this peak is identified with a depinning temperature for 2D vortex pancakes which is separate from the surface and geometrical barrier determined

irreversibility line. The depinning boundary rises steeply close to the proposed critical point² in the H - T plane and correlates closely with local Hall probe measurements.⁴ At low fields, below the melting and arrowhead fields, the temperature dependence of the FW and remanent magnetic moment exhibits a sharp change in gradient at a temperature of 32 K. Above this temperature a weaker mechanism determines the more rapid collapse of the FW and remanent magnetic moment with temperature. The locus of this low field feature adds a new boundary which appears to merge continuously with the previously identified high field depinning boundary on the H - T phase diagram. We suggest that the low field feature at 32 K may represent a depinning boundary for the 3D vortex quasilattice phase.

We are grateful to G. Balakrishnan, D. McK. Paul, T. Mochiku, and K. Kadowaki for supplying the $\text{Bi}_2\text{Sr}_2\text{CaCu}_2\text{O}_{8+\delta}$ single crystals. We would also like to thank E. Zeldov, D. E. Farrell, M. Konczykowski, A. M. Campbell, and D. A. Cardwell for many useful discussions.

-
- ¹G. Blatter, M. F. Feigelman, V. B. Geshkenbein, A. I. Larkin, and V. M. Vinokur, *Rev. Mod. Phys.* **66**, 1125 (1994).
- ²D. Majer, E. Zeldov, H. Shtrikman, and M. Konczykowski, unpublished (1996).
- ³N. Chikumoto, M. Konczykowski, N. Motohira, K. Kishio, and K. Kitazawa, *Physica C* **185-189**, 2201 (1991).
- ⁴E. Zeldov, D. Majer, M. Konczykowski, A. I. Larkin, V. M. Vinokur, V. B. Geshkenbein, N. Chikumoto, and H. Shtrikman, *Europhys. Lett.* **30**, 367 (1995).
- ⁵E. Zeldov, A. I. Larkin, V. B. Geshkenbein, M. Konczykowski, D. Majer, B. Khaykovich, V. M. Vinokur, and H. Strikman, *Phys. Rev. Lett.* **73**, 1428 (1994).
- ⁶D. Majer, Z. Zeldov, and M. Konczykowski, *Phys. Rev. Lett.* **75**, 1166 (1995).
- ⁷R. Cubitt, E. M. Forgan, G. Yang, S. L. Lee, D. McK. Paul, H. A. Mook, M. Yethiraj, P. H. Kes, T. W. Li, A. A. Menovsky, Z. Tarnawski, and K. Mortensen, *Nature (London)* **365**, 407 (1993).
- ⁸E. M. Forgan, M. T. Wylie, S. Lloyd, S. L. Lee, and R. Cubitt, *Czech. J. Phys.* **46**, 1571 (1996).
- ⁹Z. Yao, S. Yoon, H. Dai, S. Fan, and C. M. Lieber, *Nature (London)* **371**, 777 (1994).
- ¹⁰T. Giamarchi and P. Le Doussal, *Phys. Rev. B* **52**, 1242 (1995).
- ¹¹D. T. Fuchs, R. A. Doyle, E. Zeldov, D. Majer, W. S. Seow, R. J. Drost, T. Tamegai, S. Ooi, M. Konczykowski, and P. H. Kes, *Phys. Rev. B* **55**, R6156 (1997).
- ¹²R. A. Doyle, D. Liney, W. S. Seow, and A. M. Campbell, *Phys. Rev. Lett.* **75**, 4520 (1995).
- ¹³P. H. Kes, H. Pastoriza, T. W. Li, R. Cubitt, E. M. Forgan, S. L. Lee, M. Konczykowski, B. Khaykovich, D. Majer, D. T. Fuchs, and E. Zeldov, *J. Phys. I* **6**, 2327 (1996).
- ¹⁴B. Khaykovich, M. Konczykowski, E. Zeldov, R. A. Doyle, D. Majer, P. H. Kes, and T. W. Li, *Phys. Rev. B* **56**, R517 (1997).
- ¹⁵G. Balakrishnan, D. McK. Paul, M. R. Lees, and A. R. Boothroyd, *Physica C* **206**, 148 (1993).
- ¹⁶T. Mochiku and K. Kadowaki, *Trans. Mater. Res. Soc. Jpn.* **19A**, 349 (1993).
- ¹⁷C. D. Dewhurst, D. A. Cardwell, A. M. Campbell, R. A. Doyle, G. Balakrishnan, and D. McK. Paul, *Phys. Rev. B* **53**, 14 594 (1996).
- ¹⁸A. A. Zhukov, A. V. Volkov and P. A. J. de Groot, *Phys. Rev. B* **52**, 13 013 (1995).
- ¹⁹J. R. Clem and Z. D. Hao, *Phys. Rev. B* **48**, 13 774 (1993).
- ²⁰A. E. Koshelev *et al.*, *Physica C* **191**, 219 (1992).
- ²¹L. Burlachkov, V. B. Geshkenbein, A. E. Koshelev, A. I. Larkin, and V. M. Vinokur, *Phys. Rev. B* **50**, 16 770 (1994).
- ²²A. E. Koshelev, *Physica C* **223**, 276 (1994).
- ²³M. Nideröst, A. Suter, P. Visani, A. C. Mota, and G. Blatter, *Phys. Rev. B* **53**, 9286 (1996).
- ²⁴E. Zeldov, D. Majer, M. Konczykowski, V. B. Geshkenbein, V. M. Vinokur, and H. Strikman, *Nature (London)* **375**, 373 (1995).
- ²⁵B. Khaykovich, E. Zeldov, D. Majer, T. W. Li, P. H. Kes, and M. Konczykowski, *Phys. Rev. Lett.* **76**, 2555 (1996).